


Article

Design, Synthesis and Anticancer Evaluation of Substituted Cinnamic Acid Bearing 2-Quinolone Hybrid Derivatives

Ali H. Abu Almaaty ¹, Nermeen A. Elgrahy ², Eman Fayad ³, Ola A. Abu Ali ⁴, Ahmed R. E. Mahdy ⁵, Lamiaa A. A. Barakat ² and Mohammed El Behery ^{2,*}

- ¹ Zoology Department, Faculty of Science, Port Said University, Port Said 42526, Egypt; ali_zoology_2010@yahoo.com
- ² Chemistry Department (The Division of Biochemistry), Faculty of Science, Port Said University, Port Said 42526, Egypt; nermeenelgrahy291@gmail.com (N.A.E.); lamiaabarakat@yahoo.com (L.A.A.B.)
- ³ Department of Biotechnology, Faculty of Science, Taif University, P.O. Box 11099, Taif 21944, Saudi Arabia; e.esmail@tu.edu.sa
- ⁴ Department of Chemistry, College of Science, Taif University, P.O. Box 11099, Taif 21944, Saudi Arabia; O.abuali@tu.edu.sa
- ⁵ Chemistry Department (The Division of Organic Chemistry), Faculty of Science, Port Said University, Port Said 42526, Egypt; ahmed.ragab@sci.psu.edu.eg
- * Correspondence: elbehery@sci.psu.edu.eg

Abstract: A new series of hybrid molecules containing cinnamic acid and 2-quinolinone derivatives were designed and synthesized. Their structures were confirmed by ¹H-NMR, ¹³C-NMR and mass analyses. All the synthesized hybrid molecules were assessed for their in vitro antiproliferative activity against more than one cancer cell lines. Compound 3-(3,5-dibromo-7,8-dihydroxy-4-methyl-2-oxoquinolin-1(2H)-ylamino)-3-phenylacrylic acid (**5a**) with IC₅₀ = 1.89 μM against HCT-116 was proved to be the most potent compound in this study, as compared to standard drug staurosporin. DNA flow cytometry assay of compound **5a** revealed G2/M phase arrest and pre-G1 apoptosis. Annexin V-FITC showed that the percentage of early and late apoptosis was increased. The results of topoisomerase enzyme inhibition activity showed that the hybrid molecule **5a** displays potent inhibitory activity compared with control.

Keywords: 2-quinolone hybrid derivatives; cytotoxicity; apoptosis; cell cycle analysis; topoisomerase II



Citation: Abu Almaaty, A.H.; Elgrahy, N.A.; Fayad, E.; Abu Ali, O.A.; Mahdy, A.R.E.; Barakat, L.A.A.; El Behery, M. Design, Synthesis and Anticancer Evaluation of Substituted Cinnamic Acid Bearing 2-Quinolone Hybrid Derivatives. *Molecules* **2021**, *26*, 4724. <https://doi.org/10.3390/molecules26164724>

Academic Editor: Luisella Verotta

Received: 12 July 2021

Accepted: 3 August 2021

Published: 4 August 2021

Publisher's Note: MDPI stays neutral with regard to jurisdictional claims in published maps and institutional affiliations.



Copyright: © 2021 by the authors. Licensee MDPI, Basel, Switzerland. This article is an open access article distributed under the terms and conditions of the Creative Commons Attribution (CC BY) license (<https://creativecommons.org/licenses/by/4.0/>).

1. Introduction

Molecular hybridization is a commonly molecular modification approach to obtain multiple compounds with therapeutic advantages over the two different drugs [1–8]. The novel hybrid molecules have the potential to enhance efficacy, improve safety, be cost-effective and reduce the propensity to elicit resistance relative to the parent drugs [9,10]. It is therefore understandable that the investigation of new hybrid anticancer drugs has recently become of great therapeutic interest.

2-quinolones (1-azacoumarins) play an important role in anticancer drug design since their derivatives have shown excellent anticancer activity through different mechanisms such as growth inhibition via apoptosis or inhibition of angiogenesis [11–14]. Additionally, the antineoplastic activity of these quinolones was attributed to intercalating binding to DNA [15]. Moreover, 6-substituted-1-azacoumarins are under human clinical experiments as an effective oral antitumor medicine [16]. Furthermore, subsequent, introduction of hydrophilic side chain to 2-quinolone scaffold led to the discovery of topotecan and irinotecan which currently used as anticancer drugs [17].

Cinnamic acid and its natural analogues are known for the treatment of cancer for over centuries [18,19]. The hydroxy cinnamic acids are natural products arisen from the deamination of the phenyl alanine. Natural hydroxy cinnamates are extremely potent

antitumor agents [20–22]. Chemically, it is an aromatic fatty acid composed of a phenyl ring substituted with an acrylic acid group, commonly in the *trans*-geometry, and has low toxicity in human exposure. Cinnamic acid derivatives have been evaluated as pharmacologically active compounds [23]. They show a remarkable variety of biological activities and are often used as promising starting compounds for the development of new, highly effective drugs [24–26]. Cinnamic acid possesses α,β unsaturated carbonyl moiety, which can be considered as a Michael acceptor, an active moiety often employed in the design of anticancer drugs [27].

Based on the potent anticancer activity displayed by known quinolone derivatives, a new series of hybrid molecules were designed and synthesized. The hybrid structure contains cinnamic acids bearing 7,8-dihydroxy-4-methyl-1-amino-2-quinolinone as shown in Figure 1.

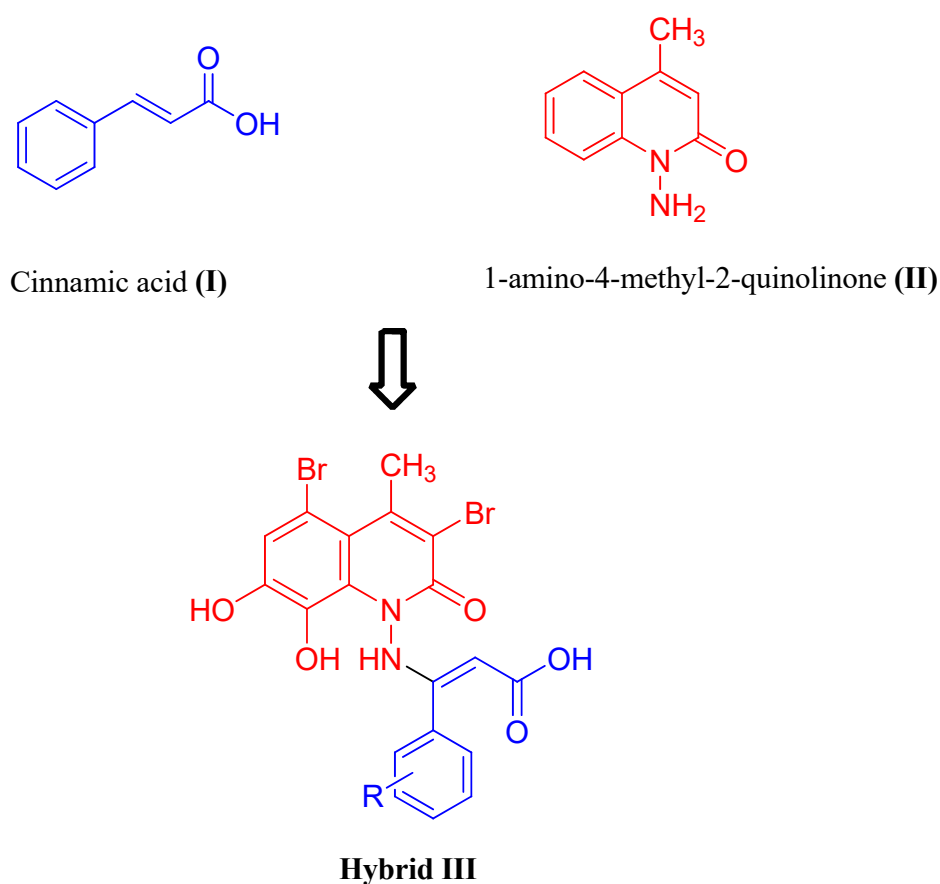


Figure 1. Molecular strategy related to cinnamic acid-2-quinolone hybrid **III** obtained from hybridization of cinnamic acid (**I**) and 1-amino-4-methyl-2-quinolinone (**II**).

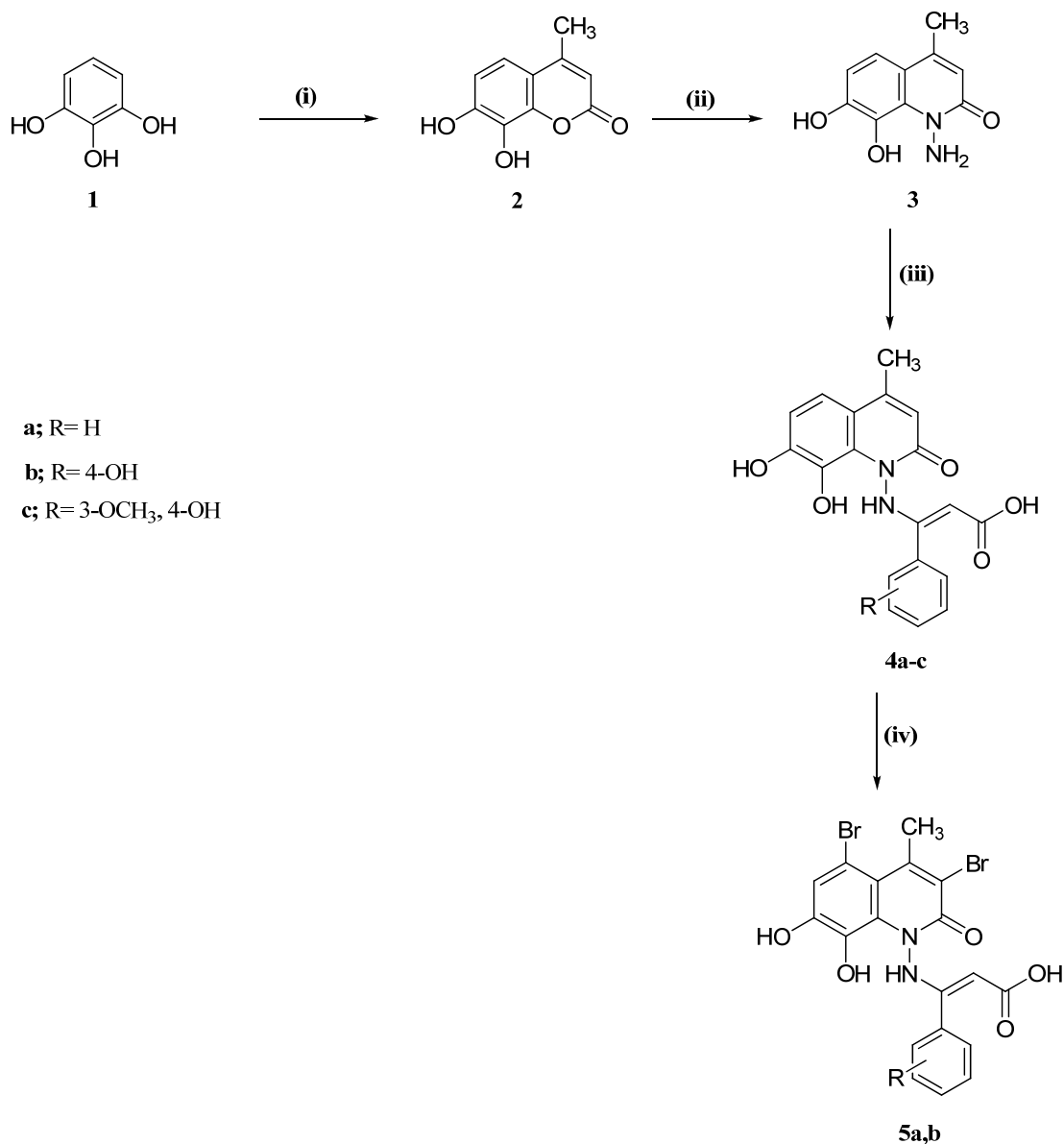
2. Results and Discussion

2.1. Chemistry

The synthetic pathway leading to the 7,8-dihydroxy-4-methyl-1-amino-quinoline-2-one (**3**) and 3-(2-oxoquinolin-1(2*H*)-ylamino)-3-arylacrylic acid derivatives **4** and **5** is outlined in Scheme 1.

7,8-dihydroxy-4-methylcoumarin (**2**) was obtained via the condensation of pyrogallol with ethyl acetoacetate in the presence of acid catalyst according to literature procedure [28]. Reaction of 7,8-dihydroxy-4-methyl-coumarin (**2**) with hydrazine hydrate in pyridine led to the formation of 1-amino-7,8-dihydroxy-4-methylquinolin-2(1*H*)-one (**3**). FT-IR spectrum of compound **3** showed the absence absorption band of carbonyl function for the coumarin ring, in addition to new absorption band at 1688 cm^{-1} due to carbonyl function of the amide group, in addition two new bands at 3225 , and 3178 cm^{-1} related to NH_2 group.

$^1\text{H-NMR}$ spectrum of compound **3** showed characteristic two singlet signals at δ 2.35 and 6.12 ppm due to the protons of methyl group (CH_3) and H-3 of quinolinone ring. Protons of the aromatic ring were appeared at δ 6.82 and 7.10 as doublet signal of H-5 and H-6 for the quinolinone ring. The $^{13}\text{C-NMR}$ spectrum of compound **3** showed four carbon signals at δ 160.73, 154.44, 150.01 and 143.75 ppm assigned to carbonyl function ($\text{C}=\text{O}$), two carbons (C-O) and one carbon (C-N) groups.



Scheme 1. Synthesis of 3-(2-oxoquinolin-1(2H)-ylamino)-3-arylacrylic acid (**4** and **5**). Reagents and reaction condition: (i) $\text{CH}_3\text{COCH}_2\text{COOEt}$, conc H_2SO_4 , (ii) N_2H_4 , pyridine; (iii) Ar-CH=CH-COOH , NaOAc , (iv) Br_2 , AcOH .

Treatment of 1-amino-7,8-dihydroxy-4-methylquinolin-2(1H)-one (**3**) with substituted cinnamic acids in refluxing ethanol in the presence of fused sodium acetate provided the corresponding 3-(7,8-dihydroxy-4-methyl-2-oxoquinolin-1(2H)-ylamino)-3-arylacrylic acid **4a-c**.

The structure of compounds **4a-c** has been described by IR, $^1\text{H-NMR}$ and $^{13}\text{C-NMR}$. The IR spectrum of compound **4a** as representative example, revealed the presence of two stretching vibration bands for NH and carbonyl of acid at 3232 and 1695 cm^{-1} , respectively. The $^1\text{H-NMR}$ spectrum of compound **4a** showed additional signals in the region δ 6.52–7.69 ppm with the presence of aromatic, olefinic and NH protons. In addition, the

^{13}C -NMR spectrum of compound **4a** showed three signals at δ 168.31, 160.74 and 18.73 ppm assigned to the carbons of two carbonyl and methyl groups, respectively. In addition, the ^{13}C -NMR spectrum of compound **4a** displayed an additional carbon signals in the region of δ 134.77–110.62 ppm attributed to the carbons of quinoline, aromatic and olefinic carbons.

The halogenation of compounds **4a,b** with bromine in glacial acetic with stirring at 60 °C led to the formation of 3-(3,5-dibromo-7,8-dihydroxy-4-methyl-2-oxoquinolin-1(2H)-ylamino)-3-arylacrylic acid **5a,b**. In the ^1H -NMR spectrum of compound **5a** Protons of the aromatic and H-6 of quinolinone ring were observed as multiplet signals within the expected chemical shift region at δ 7.35–7.69 ppm. The ^{13}C -NMR spectrum of **5a** showed four carbons appeared as four signals at δ 152.09, 147.53, 144.41 and 141.54 ppm due to two carbons of C-O and C-N groups. In addition, carbons of the aromatic and quinolinone rings were observed a characteristic carbon signals in the region δ 138.68–107.12 ppm.

2.2. Evaluation of Biological Activity

2.2.1. In Vitro Cytotoxic Activity against Three Cancer Cell Line

The effect of quinolone derivatives **3**, **4a,b** and **5a,b** on the viability of three cancer cell lines were studied using MTT assay (Table 1). The cytotoxicity was assessed using Staurosporin (STU) as positive control. The three cancer cell lines are MCF-7 (breast cancer cell line), HepG2 (hepatocellular carcinoma cell line) and colon carcinoma (HCT-116). The obtained results indicated that compound **5b** exhibited the most potent cytotoxic activity against MCF-7 cells with IC_{50} value 8.48 μM . In addition, compound **5a** exhibited potential cytotoxic activity against HepG2 and HCT-116 cells with IC_{50} values 4.05 and 1.89 μM , respectively. From the obtained results it can be concluded that, the presence of bromine at C3 and C5 of quinolone ring has better anticancer activity against three cancer cell lines.

Table 1. In vitro antitumor activity of quinolone derivatives **3**, **4a,b** and **5a,b** over MCF-7, HepG2 and HCT-116, cell lines. Data are expressed as the mean \pm SD.

Comp No.	IC_{50} (μM)		
	MCF-7	HepG2	HCT-116
3	32.9 \pm 1.81	8.23 \pm 0.42	15.0 \pm 0.79
4a	18.7 \pm 1.03	19.4 \pm 0.99	21.3 \pm 1.12
4b	11.8 \pm 0.65	15.5 \pm 0.79	7.56 \pm 0.4
5a	19.3 \pm 1.06	4.05 \pm 0.21	1.89 \pm 0.10
5b	8.48 \pm 0.47	30.9 \pm 1.57	10.7 \pm 0.57
STU	6.91 \pm 0.38	5.23 \pm 0.27	4.25 \pm 0.22

2.2.2. Cell Cycle Analysis

Targeting the cell cycle of tumor cells has been recognized as a promising strategy for cancer therapy [29,30]. In this study, cell cycle analysis was followed via DNA flow cytometric analysis using propidium iodide (PI) as staining agent following hybrid molecule **5a** treatment at its IC_{50} concentration for 48 h. The results showed that the tested compound increase the percentage of cell population at G2/M phase by 2.83-fold compared to untreated control group. While the number of cells in the G1 and S phases were reduced. Additionally, the result showed that compound **5a** increased the percentage of cells at pre-G1 phase by 8.29-fold compared to the control (Figure 2).

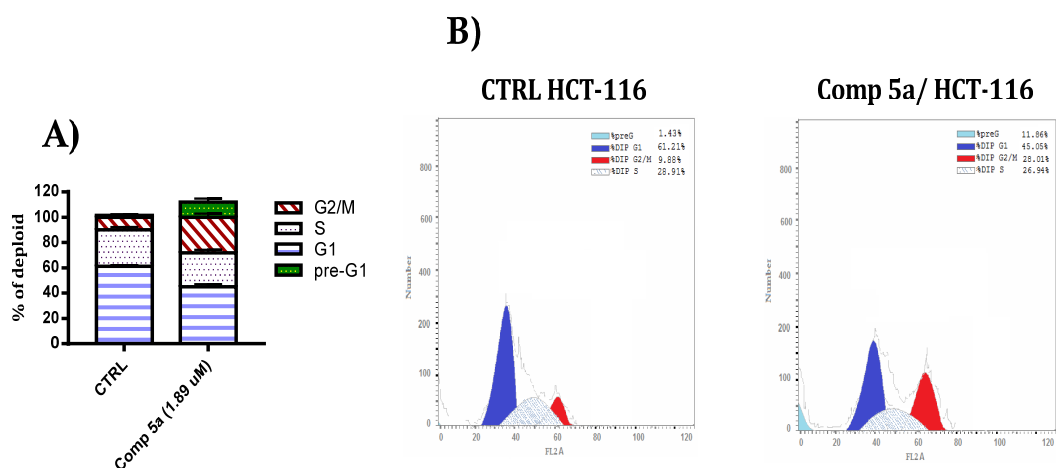


Figure 2. (A) Graphical representation of cell cycle distribution of HCT-116 cell line induced by compound 5a. (B) Cell cycle distribution of HCT-116 cell line induced by compound 5a.

2.2.3. Apoptosis Detection Assay

To characterize the mode of cell death caused by compound 5a, a biparametric cytofluorimetric analysis using PI and Annexin-V-FITC was performed in HCT-116 cells after treatment with compound 5a at its IC_{50} concentration dose value for 48 h (Figure 3). The results revealed that compound 5a increases in the percentage of total apoptosis compared with untreated control group. The percentage of early apoptosis was increased from 0.71% to 6.65% compared with the untreated control group. Additionally, compound 5a can increase the percentage of late apoptosis from 0.52% to 7.87% compared with untreated control.

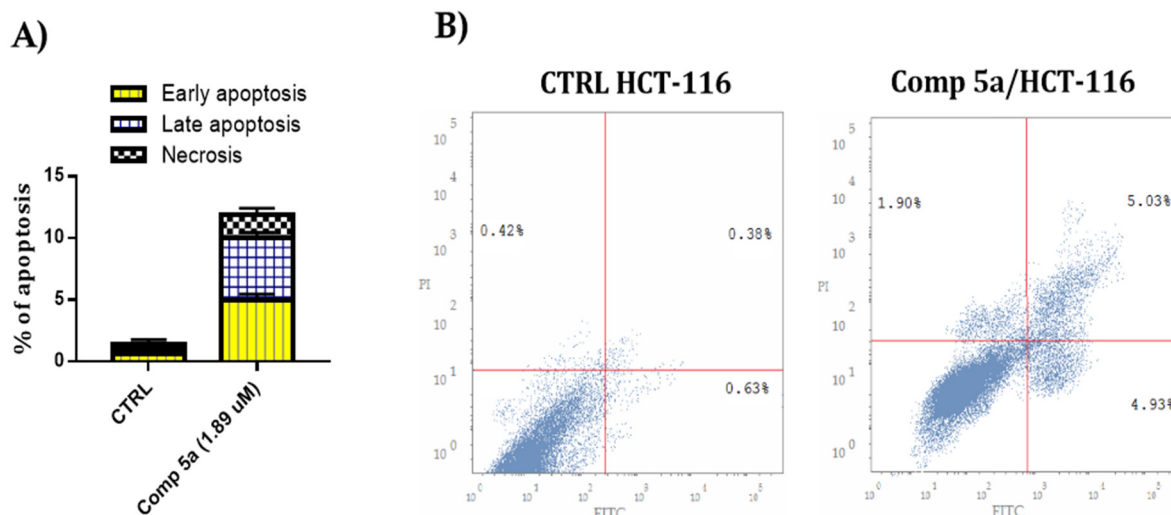


Figure 3. (A) Graphical representation of apoptosis effect of compound 5a on HCT-116 cell line. (B) Apoptosis effect of compound 5a on HCT-116 cell line.

2.2.4. Topoisomerase II Inhibitory Activity

Compound 5a was evaluated for inhibitory activity on Topoisomerase II (topo II). Five dose concentrations were used and IC_{50} concentration was determined. Podophyllotoxin (podo) was employed as the standard. It is observed that, compound 5a revealed strong inhibitory activity against topo II with IC_{50} value of 75.82 ng/mL, compared to the reference compound podo ($IC_{50} = 31.24$ ng/mL) (Figure 4).

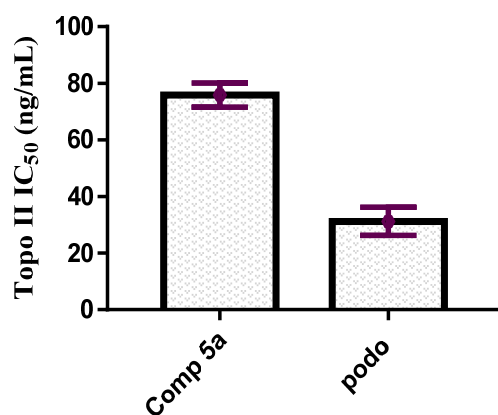


Figure 4. Graphical presentation for comparison of topo II IC₅₀ (ng/mL) of the compound 5a and podo.

2.3. Molecular Docking Study

Molecular docking is a vital tool in drug design [31–34]. Molecular docking achieves a confirmation for the protein and ligand interactions. In this work, molecular docking was conducted using the synthesized compounds (3, 4a,b, and 5a,b) against breast cancer protein (PDB: 3HB5). The docking results showed a potential structure-activity relationship between the target compounds (3, 4a,b, and 5a,b) against 3HB5 protein as shown in (Table 2, Figures 5 and 6). Compounds 4a and 5a showed the highest binding interaction against the key amino acids of the 3HB5 with docking scores -9.8 and -9.56 kcal.mol⁻¹ respectively. The binding affinity and interaction bonds between docked compounds and active site of target protein 3HB5 were hydrogen bond, polar and hydrophobic interaction as shown in (Table 2). Compounds 5a exhibited a potential interaction toward (3HB5) receptor which is compatible with cytotoxicity and biological results.

Table 2. Docking scores of synthesized compounds (3, 4a,b, and 5a,b) against 3HB5 (PDB: 3HB5).

Comp No.	Docking Scores (kcal.mol ⁻¹)	Hydrogen Bonds	Polar Interaction	Hydrophobic Interactions
3	-6.42	ASN90	LYS159 SER12	PHE192 ILE14
4a	-9.81	LYS195 SER142		PHE192 ILE14 PHE226
4b	-7.56	PHE192	SER12 ASN90 LYS195 THR190 GLY141 VAL188	ILE14
5a	-9.56	THR190	SER142 TYR155	PHE192 ILE14
5b	-6.06	GLY92 SER12 ASN90 SER11	ARG37 THR190	ALA191

3.1.1. Synthesis of 7,8-Dihydroxy-4-methyl Coumarin (2)

A mixture of pyrogallol (0.01 mol) and ethyl acetoacetate (0.01 mol) in the presence of concentrated sulfuric acid (2 mL) as acid catalyzed was heated under reflux on a water bath for 2 h. The reaction mixture was cooled and poured into water, the solid formed was filtered off, washed with water and dried. Finally, the product was crystallized from hot water.

7,8-Dihydroxy-4-methyl coumarin (**2**, known). IR (KBr) ν_{\max} : 3458 (br. OH), 1725 (C=O), 1605, 1583 (C=C), 1170, 1065, 1035 (C-O) cm^{-1} . $^1\text{H-NMR}$ (DMSO- d_6) δ : 2.34 (s, 3H, CH₃), 6.21 (s, 1H, H-3 of coumarin ring), 6.91 (d, 1H, H-6 of coumarin ring), 7.21 (d, 1H, H-5 of coumarin ring), 9.68 (br. s, 1H, OH), 9.14 (br. s, 1H, OH) ppm. MS (m/z , %) = 192 (M^+ , 76.30). Anal. Calcd. for C₈H₈O₄ (192): C, 62.50; H, 4.17. Found: C, 62.33; H, 4.03.

3.1.2. Synthesis of 1-Amino-7,8-dihydroxy-4-methylquinolin-2(1H)-one (3)

A solution of 7,8-dihydroxy-4-methyl coumarin (0.01 mol) in pyridine (30 mL) was added hydrazine hydrate (0.02 mol), then heating under reflux for 6 h. The reaction mixture was cooled, poured into ice-water and neutralized with dilute hydrochloric acid (1N). The solid obtained was filtered off, washed with water, dried and purified by crystallization from absolute ethanol.

1-Amino-7,8-dihydroxy-4-methylquinolin-2(1H)-one (**3**) as yellow crystals, yield 71%, m.p. 265–267 °C. IR (K Br) ν_{\max} : 3418 (br OH), 3225, 3178 (NH₂), 1648 (C=O), 1619, 1587 (C=C), 1061, 1006 (C-O) cm^{-1} . $^1\text{H-NMR}$ (DMSO- d_6) δ : 2.35 (s, 3H, CH₃), 4.12 (br.s, 2H, NH₂), 6.12 (s, 1H, H-3 of quinolinone), 6.82 (d, 1H, H-6 of quinolinone), 7.09 (d, 1H, H-5 of quinolinone) ppm. $^{13}\text{C-NMR}$ (DMSO- d_6) δ : 160.73 (C-2), 154.44 (C-7), 150.01 (C-8), 143.75 (C-9), 132.69 (C-4), 115.92 (C-10), 113.17 (C-5), 112.60 (C-6), 110.59 (C-3), 18.73 (C-11) ppm. MS (m/z , %) = 206 (M^+ , 17.30). Anal. Calcd. for C₁₀H₁₀N₂O₂ (206): C, 58.25; H, 4.85; N, 13.59. Found: C, 58.09; H, 4.66; N, 13.39.

3.1.3. Synthesis of 3-(7,8-Dihydroxy-4-methyl-2-oxoquinolin-1(2H)-ylamino)-3-arylacrylic Acid (4a–c)

A suspension of a suitable cinnamic acid derivative (0.01 mol) and 1-amino-7,8-dihydroxy-4-methylquinolin-2(1H)-one (**3**, 0.01 mol) in ethanol (30 mL), in the presence of fused sodium acetate (0.03 mol) was refluxed for 4 h. The reaction mixture was cooled down, poured into water, and the solid formed was filtered. The product was crystallized from a suitable solvent to give compound **4a–c**.

3-(7,8-dihydroxy-4-methyl-2-oxoquinolin-1(2H)-ylamino)-3-phenylacrylic acid (**4a**) Pale yellow crystals, yield 76%, m.p. 185–187 °C. Crystallized from ethanol/H₂O (3:1). IR (KBr) ν_{\max} : 3550–3350 (br. OH), 3232 (NH), 1705–1675 (br. C=O), 1629, 1584 (C=C), 1229, 1061, 1006 (C-O) cm^{-1} . $^1\text{H-NMR}$ (DMSO- d_6) δ : 2.36 (s, 3H, CH₃), 6.13 (s, 1H, H-3 of quinolinone), 6.56 (s, 1H, H-olefinic of cinnamic acid), 6.38 (d, 1H, H-6 of quinoline ring), 7.10 (d, 1H, H-5 of quinolinone ring), 7.41–7.69 (m, 6H, Ar-H and NH) ppm. $^{13}\text{C-NMR}$ (DMSO- d_6) δ : 168.31 (C-21), 160.74 (C-7), 150.00 (C-8), 144.11 (C-9), 143.82 (C-13), 134.77 (C-17), 132.72 (C-4), 130.62 (C-14), 129.37 (C-15,9), 128.63 (C-16,18), 120.09 (C-20), 115.92 (C-10), 113.21 (C-5), 112.67 (C-6), 110.62 (C-3), 18.73 (C-H) ppm. MS (m/z , %) = 352 (M^+ , 13.51). Anal. Calcd. for C₁₉H₁₆N₃O₅ (352), C, 64.77; H, 4.54; N, 7.95. Found: C, 64.58; H, 4.33; N, 7.77.

3-(7,8-Dihydroxy-4-methyl-2-oxoquinolin-1(2H)-ylamino)-3-(4-hydroxyphenyl)acrylic acid (**4b**) Pale yellow crystals, yield 69%, m.p. 181–183 °C. Crystallized from ethanol/H₂O (3:1). IR (KBr) ν_{\max} : 3560–3100 (br. OH), 3232 (NH), 1701–1660 (C=O), 1626, 1593 (C=C), 1170, 1062, 1007 (C-O) cm^{-1} . $^1\text{H-NMR}$ (DMSO- d_6) δ : 2.35 (s, 3H, CH₃), 6.12 (s, 1H, H-3 of quinolinone ring), 6.28–7.53 (m, 8H, Ar-H, olefinic and NH) ppm. $^{13}\text{C-NMR}$ (DMSO- d_6) δ : 168.45 (C-21), 160.70 (C-2), 160.70 (C-17), 154.39 (C-7), 149.87 (C-8), 144.65 (C-9), 143.79 (C-13), 132.63 (C-4), 130.56 (C-15,19), 125.74 (C-14), 116.22 (C-16,18), 115.95 (C-10), 115.81 (C-20), 113.24 (C-5), 112.60 (C-6), 110.66 (C-3), 18.71 (C-11) ppm. MS (m/z , %) = 368 (M^+ ,

11.51). Anal. Calcd. for $C_{19}H_{16}N_2O_6$ (368): C, 61.96; H, 3.35; N, 7.61. Found: C, 61.73; H, 3.11; N, 7.51.

3-(7,8-Dihydroxy-4-methyl-2-oxoquinolin-1(2H)-ylamino)-3-(4-hydroxy-3-methoxyphenyl) acrylic acid (**4c**). Pale yellow crystals, yield 67%, m.p. 175–177 °C. Crystallized from DMF/H₂O (1:1). IR (KBr) ν_{\max} : 3550–2984 (br. OH), 3232 (NH), 1700–1652 (C=O), 1620, 1595 (C=C), 1172, 1141, 1062 (C-O) cm^{-1} . ¹H-NMR (DMSO-*d*₆) δ : 2.35 (s, 3H, CH₃), 3.82 (s, 3H, OCH₃), 6.12 (s, 1H, H-3 of quinolinone ring), 6.36–7.52 (m, 7H, Ar-H, H-olefinic and NH), 9.35 (br.s, 1H, OH), 10.02 (br.s, 2H, 2xOH) ppm. ¹³C-NMR (DMSO-*d*₆) δ : 168.51 (C-21), 160.70 (C-2), 154.41 (C-7), 149.87 (C-8), 149.53 (C-17), 148.37 (C-18), 144.99 (C-9), 143.78 (C-13), 132.26 (C-4), 126.23 (C-15), 123.21 (C-19), 116.10 (C-10), 115.95 (C-14,16), 113.23 (C-5), 112.58 (C-6), 111.56 (C-20), 110.65 (C-3), 56.13 (C-22), 18.72 (C-11) ppm. MS (*m/z*, %) = 398 (M⁺, 8.60). Anal. Calcd. for $C_{20}H_{18}N_2O_7$ (398): C, 60.30; H, 4.52; N, 7.03. Found: C, 60.11; H, 4.29; N, 6.89.

3.1.4. Synthesis of 3-(3,5-Dibromo-7,8-dihydroxy-4-methyl-2-oxoquinolin-1(2H)-ylamino)-3-arylacrylic Acid (**5a,b**)

In 15 mL of glacial acetic acid, compound **4** (0.01 mol) was dissolved. Then, 10 mL of bromine (0.02 mol) in glacial acetic acid was added dropwise to compound **4** solution with stirring at 60 °C. After 5–10 min. the bromine color was discharged and a yellow solution remained. At this point, an additional 0.5–1 mL of the bromine-AcOH solution was added with stirring at room temperature for 30–45 min. The reaction mixture was poured into water and the resulting product was filtered off, washed with water and dried. Finally, The product was crystallized from DMF/H₂O (1:1) to give **5a,b**.

3-(3,5-Dibromo-7,8-dihydroxy-4-methyl-2-oxoquinolin-1(2H)-ylamino)-3-phenylacrylic acid (**5a**) Yellow crystals, yield 71%, m.p. 225–227 °C. IR(KBr) ν_{\max} : 3452 (br. OH), 3254 (NH), 1710–1705 (C=O), 1627, 1604, 1558 (C=C), 1223, 1072, 1026 (C-O) cm^{-1} . ¹H-NMR (DMSO-*d*₆) δ : 2.55 (s, 3H, CH₃), 5.32 (d, 1H, H-olefinic) 5.54 (d, 1H, H-olefinic of two isomer), 6.54 (d, 1H, NH), 7.38–7.69 (m, 6H, Ar-H for two isomer) 10.35 (br.s, 1H, OH), 10.53 (br.s, 1H, OH) ppm. ¹³C-NMR (DMSO-*d*₆) δ : 169.56, 168.05 (C=O of acid for two isomer), 156.46 (C-2), 152.09, 147.5, (C-O), 144.41, 141.54 (C-N), 138.68, 134.67, 133.30, 130.68, 129.54, 129.35, 129.15, 128.65, 128.65, 119.66, 119.38, 113.62, 109.24, 107.12 (C-aromatic acid Quinolinone ring), 52.38, 47.69 (C-olefinic), 20.01 (CH₃) ppm. MS (*m/z*, %) = 508(M⁺, unstable). Anal. Calcd. for $C_{19}H_{14}N_2Br_2O_5$ (508): C, 44.88, H, 2.75; N, 5.51. Found: C, 44.64; H, 2.52; N, 5.33.

3-(3,5-dibromo-7,8-dihydroxy-4-methyl-2-oxoquinolin-1(2H)-ylamino)-3-(4-hydroxyphenyl) acrylic acid (**5b**). Pale yellow crystals, yield 69%, m.p. 233–235 °C. IR (KBr) ν_{\max} : 3580–2955 (br. OH and NH), 1717–1705 (br. C=O), 1607, 1558 (C=C), 1239, 1160, 1101, 1028 (C-O) cm^{-1} . ¹H-NMR (DMSO-*d*₆) δ : 2.53 (s, 3H, CH₃), 7.01–8.16 (m, 6H, Ar-H and H-olefinic) ppm. ¹³C-NMR (DMSO-*d*₆) δ : 166.21, 156.46 (C=O), 152.08, 151.84, 151.04 (C-O), 147.52, 141.53 (C-N), 134.49, 134.31, 133.31, 132.87, 132.46, 130.87, 130.77, 130.23, 119.36, 116.83, 113.61, 112.63, 112.34, 111.94, 109.24, 108.50, 107.78, 106.22 (C-Quinolinone, aromatic and olefinic carbons), 20.16, 20.01 (CH₃, two isomer). MS: (*m/z*, %) = 524(M⁺, unstable). Anal. Calcd. for $C_{19}H_{14}N_2Br_2O_6$ (524): C, 43.51; H, 2.67; N, 5.34. Found: C, 43.34; H, 2.42; N, 5.51. ¹H and ¹³C NMR of compound **3**, **4a–c** and **5a–b** are available in Supplementary Materials.

3.2. Biological Evaluation

3.2.1. Anti-Tumor Activity against Three Cancer Cell Lines

The cytotoxic activity was measured in vitro using the MTT assay. Cells were plated in 96-multiwell plate (10⁵ cells/well) for 24 h before treatment with the compounds. Test compounds were dissolved in dimethyl sulfoxide (DMSO) which did not exceed 1% final concentration. Different concentrations of the compound under test (0.39, 1.56, 6.25, 25, and 100 μ g/mL) were added to the cell's monolayer. Triplicate wells were prepared for each individual concentration. Monolayer cells were incubated with the compound(s) for 48 h

at 37 °C and in atmosphere of 5% CO₂. After 48 h, cells were fixed, washed with phosphate buffer saline (PBS, pH = 7.4) and stained with 40 µL of MTT solution (5 mg/mL of MTT in 0.9% NaCl) in each well was added and incubated for an additional 4 h. MTT crystals were solubilized by adding 180 µL of acidified isopropanol/well and the plate was shaken at room temperature, followed by photometric determination of the absorbance at 570 nm using ELISA reader. The molar concentration required to inhibit 50% of cell viability (IC₅₀) was calculated and compared with the reference drug STU. The surviving fractions were expressed as means ± SD.

3.2.2. Cell Cycle Analysis of Compound 5a

HCT-116 cells, (3.0×10^5 cells/well) and incubated at 37 °C for 12 h. The target cells were then treated with the compound 5a at its IC₅₀ concentration dose value for 48 h. After treatment, cells were collected and fixed with 75% ethanol at 20 °C overnight, then, cells were washed with PBS followed by centrifugation and incubated with (10 mg/mL) Rnase (Sigma, St. Louis, MO, USA) and (5 mg/mL) propidium iodide (PI, Sigma) before flow cytometry analysis (FACSCalibur cytometer using Cellquest software, BD Bioscience, San Jose, CA, USA).

3.2.3. Apoptosis Determination by Annexin-V Assay

The HCT-116 cells (2×10^5 /well) were treated with compound 5a at its IC₅₀ concentration value for 48 h. After treatment, cells were harvested and washed twice (180 g, 10 min, 4 °C) with PBS. Each cell well was resuspended in 100 µL of binding buffer, and 5 µL Annexin V-FITC were added. After an incubation time of 10 min at room temperature, additional 400 µL of binding buffer were added for a final volume of 500 µL. Cells were stained with PI immediately before measurement. Cells were the analyzed by using *FACS Calibur* Flow cytometer (Becton and Dickinson, Heidelberg, Germany). Data thus obtained were analyzed with Cell-Quest software (Becton and Dickinson, Heidelberg, Germany).

3.2.4. In Vitro Topoisomerase Inhibitory Assay

Compound 5a was selected to be evaluated against topoisomerase II [MBS#942146] using human DNA topoisomerase 2-β (TOP2β) ELISA kit according to manufacturer's instructions. Prepare all reagents, working standards, and samples. Add 100 µL of standard and sample per well and incubate for 2 h at 37 °C. Remove the liquid of each well, do not wash. Add 100 µL of biotin-antibody to each well and incubate for 1 h at 37 °C. Aspirate each well and wash three times. Add 100 µL of horseradish peroxidase (HRP-avidin) to each well and incubate for 1 h at 37 °C. Repeat the aspiration/wash process for five times. Add 90 µL of 3,3',5,5'-tetramethylbenzidine (TMB) substrate to each well and incubate for 15–30 min at 37 °C, protect from light. Add 50 µL of stop solution to each well and determine the optical density of each well within 5 min, using a microplate reader set to 450 nm. The values of % activity versus a series of compound concentrations (2.5, 5, 10, and 15 µM) were then plotted using non-linear regression analysis of sigmoidal dose-response curve. The IC₅₀ values for compound 5a against topoisomerase II was determined by the concentration causing a half-maximal percent activity and the data were compared with Dox as standard.

3.3. Molecular Docking Study

Docking calculations were estimated using a Docking Server [35]. Docking scores were examined on the 3HB5 protein model. Crucial hydrogen atoms, Kollman united atom type charges, and solvation parameters were inserted with the support of AutoDock tools. Affinity (grid) maps of 61 × 61 × 61 points and 0.375 Å spacing were created using the Autogrid program [36]. AutoDock parameter set and distance-dependent dielectric purposes were utilized in the calculation of the van der Waals and the electrostatic terms, correspondingly. Docking simulations were done via the Lamarckian genetic algorithm (LGA) and the Solis and Wets local search approach [37]. The initial position, orientation,

and torsions of the ligand molecules were fixed arbitrarily. Wholly rotatable torsions were discharged throughout docking. Each docking experimentation was originated from 2 different runs that were established to end afterward a maximum of 250,000 energy evaluations. The population size was set to 150. Throughout the search, a translational step of 0.2 Å, and quaternion and torsion steps of 5 were applied.

4. Conclusions

In conclusion, hybrid molecules containing cinnamic acid and 2-quinolinone derivatives (**4a–c**) were synthesized via the reaction of cinnamic acid derivatives with 1-amino-7,8-dihydroxy-4-methylquinolin-2(1H)-one (**3**), which was obtainable in the reaction of 7,8-hydroxy-4-methylcoumarin (**2**) with hydrazine hydrate in pyridine. Brominated derivatives **5a,b** were prepared via the halogenation of compounds **4a,b** with bromine in glacial acetic acid. Cinnamic acids bearing 2-quinolone **4a,b** and their brominated derivatives **5a,b** were assessed for their in vitro antiproliferative activity against three cancer cell lines and the brominated derivatives were found to be more active. DNA flow cytometry assay of compound **5a** revealed G2/M phase arrest and pre-G1 apoptosis. Annexin V-FITC showed the percentage of early and late apoptosis was increased. The results of topoisomerase enzyme inhibition activity showed that the hybrid molecule **5a** display potent inhibitory activity compared with control. In conclusion, the preliminary study of the anticancer activity of the prepared compounds represents a novel strategy for the discovery of anticancer compounds which needs further investigation.

Supplementary Materials: The following are available online: ¹H and ¹³C NMR of compound **3**, **4a–c** and **5a,b**.

Author Contributions: All authors participated in the production of the article. All authors have read and agreed to the published version of the manuscript.

Funding: This work was supported by Taif University Researchers Supporting project number (TURSP-2020/220), Taif University, Taif, Saudi Arabia.

Institutional Review Board Statement: Not applicable. Studies not involving humans or animals. Biological and cytotoxicity experiments were conducted on in vitro cancer cell lines.

Informed Consent Statement: Not applicable.

Data Availability Statement: Not applicable.

Acknowledgments: Taif University Researchers Supporting Project number (TURSP-2020/220), Taif University, Taif, Saudi Arabia.

Conflicts of Interest: The authors declare no conflict of interest.

Sample Availability: Samples of compounds are not available from authors.

References

1. Yu, B.; Qi, P.-P.; Shi, X.-J.; Huang, R.; Guo, H.; Zheng, Y.-C.; Yu, D.-Q.; Liu, H.-M. Efficient synthesis of new antiproliferative steroidal hybrids using the molecular hybridization approach. *Eur. J. Med. Chem.* **2016**, *117*, 241–255. [[CrossRef](#)] [[PubMed](#)]
2. Reddyrajula, R.; Dalimba, U.; Kumar, S.M. Molecular hybridization approach for phenothiazine incorporated 1,2,3-triazole hybrids as promising antimicrobial agents: Design, synthesis, molecular docking and in silico ADME studies. *Eur. J. Med. Chem.* **2019**, *168*, 263–282. [[CrossRef](#)] [[PubMed](#)]
3. Mourad, E.; Rizzk, Y.W.; Zaki, I.; Mohammed, F.Z.; el Behery, M. Synthesis and cytotoxicity screening of some synthesized hybrid nitrogen molecules as anticancer agents. *J. Mol. Struct.* **2021**, *1242*, 130722. [[CrossRef](#)]
4. Solomon, V.R.; Pundir, S.; Lee, H. Examination of novel 4-aminoquinoline derivatives designed and synthesized by a hybrid pharmacophore approach to enhance their anticancer activities. *Sci. Rep.* **2019**, *9*, 1–17. [[CrossRef](#)]
5. Khwaza, V.; Mlala, S.; Oyediji, O.O.; Aderibigbe, B.A. Pentacyclic Triterpenoids with Nitrogen-Containing Heterocyclic Moiety, Privileged Hybrids in Anticancer Drug Discovery. *Molecules* **2021**, *26*, 2401. [[CrossRef](#)]
6. Shagufta; Ahmad, I. An insight into the therapeutic potential of quinazoline derivatives as anticancer agents. *MedChemComm* **2017**, *8*, 871–885. [[CrossRef](#)] [[PubMed](#)]
7. Abbot, V.; Sharma, P.; Dhiman, S.; Noolvi, M.N.; Patel, H.M.; Bhardwaj, V. Small hybrid heteroaromatics: Resourceful biological tools in cancer research. *RSC Adv.* **2017**, *7*, 8313–28349. [[CrossRef](#)]

8. Fortin, S.; Bérubé, G. Advances in the development of hybrid anticancer drugs. *Expert Opin. Drug Discov.* **2013**, *8*, 1029–1047. [[CrossRef](#)]
9. Ramprasad, J.; Sthalam, V.K.; Thampunuri, R.L.M.; Bhukya, S.; Ummanni, R.; Balasubramanian, S.; Pabbaraja, S. Synthesis and evaluation of a novel quinoline-triazole analogs for antitubercular properties via molecular hybridization approach. *Bioorg. Med. Chem. Lett.* **2019**, *29*, 126671. [[CrossRef](#)]
10. Karthikeyan, C.; Solomon, V.R.; Lee, H.; Trivedi, P. Design, synthesis and biological evaluation of some isatin-linked chalcones as novel anti-breast cancer agents: A molecular hybridization approach. *Biomed. Prev. Nutr.* **2013**, *3*, 325–330. [[CrossRef](#)]
11. Mohamed, M.F.; Abuo-Rahma, G.E.-D.A. Molecular targets and anticancer activity of quinoline–chalcone hybrids: Literature review. *RSC Adv.* **2020**, *10*, 31139–31155. [[CrossRef](#)]
12. Elbastawesy, M.A.I.; Ramadan, M.; El-Shaier, Y.A.M.M.; Aly, A.A.; Abuo-Rahma, G.E.-D.A. Arylidene of Quinolin-2-one scaffold as Erlotinib analogues with activities against leukemia through inhibition of EGFR TK/STAT-3 pathways. *Bioorg. Chem.* **2020**, *96*, 103628. [[CrossRef](#)]
13. Huang, H.-W.; Bow, Y.-D.; Wang, C.-Y.; Chen, Y.-C.; Fu, P.-R.; Chang, K.-F.; Wang, T.-W.; Tseng, C.-H.; Chen, Y.-L.; Chiu, C.-C. DFIQ, a Novel Quinoline Derivative, Shows Anticancer Potential by Inducing Apoptosis and Autophagy in NSCLC Cell and In Vivo Zebrafish Xenograft Models. *Cancers* **2020**, *12*, 1348. [[CrossRef](#)] [[PubMed](#)]
14. Iqbal, J.; Ejaz, S.A.; Khan, I.; Ausekle, E.; Miliutina, M.; Langer, P. Exploration of quinolone and quinoline derivatives as potential anticancer agents. *DARU J. Pharm. Sci.* **2019**, *27*, 613–626. [[CrossRef](#)]
15. Bush, N.G.; Diez-Santos, I.; Abbott, L.R.; Maxwell, A. Quinolones: Mechanism, Lethality and Their Contributions to Antibiotic Resistance. *Molecules* **2020**, *25*, 5662. [[CrossRef](#)] [[PubMed](#)]
16. Singh, K.; Verma, V.; Yadav, K.; Sreekanth, V.; Kumar, D.; Bajaj, A.; Kumar, V. Design, regioselective synthesis and cytotoxic evaluation of 2-aminoimidazole–quinoline hybrids against cancer and primary endothelial cells. *Eur. J. Med. Chem.* **2014**, *87*, 150–158. [[CrossRef](#)]
17. Marzi, L.; Sun, Y.; Shar-yin, N.H.; James, A.; Difilippantonio, S.; Pommier, Y. The indenoisoquinoline LMP517: A novel antitumor agent targeting both TOP1 and TOP2. *Mol. Cancer Ther.* **2020**, *19*, 1589–1597. [[CrossRef](#)]
18. Ruwizhi, N.; Aderibigbe, B.A. Cinnamic Acid Derivatives and Their Biological Efficacy. *Int. J. Mol. Sci.* **2020**, *21*, 5712. [[CrossRef](#)]
19. Graminha, A.E.; Honorato, J.; Dulcey, L.L.; Godoy, L.R.; Barbosa, M.F.; Cominetti, M.R.; Menezes, A.C.; Batista, A.A. Evaluation of the biological potential of ruthenium(II) complexes with cinnamic acid. *J. Inorg. Biochem.* **2020**, *206*, 111021. [[CrossRef](#)]
20. Coman, V.; Vodnar, D.C. Hydroxycinnamic acids and human health: Recent advances. *J. Sci. Food Agric.* **2020**, *100*, 483–499. [[CrossRef](#)]
21. Sova, M.; Saso, L. Natural Sources, Pharmacokinetics, Biological Activities and Health Benefits of Hydroxycinnamic Acids and Their Metabolites. *Nutrients* **2020**, *12*, 2190. [[CrossRef](#)]
22. Della Pelle, F.; Rojas, D.; Silveri, F.; Ferraro, G.; Fratini, E.; Scroccarello, A.; Escarpa, A.; Compagnone, D. Class-selective voltammetric determination of hydroxycinnamic acids structural analogs using a WS2/catechin-capped AuNPs/carbon black-based nanocomposite sensor. *Microchim. Acta* **2020**, *187*, 296. [[CrossRef](#)] [[PubMed](#)]
23. Romanov, S.; Aksunova, A.; Bakhtiyarova, Y.; Shulaeva, M.; Pozdeev, O.; Egorova, S.; Galkina, I.; Galkin, V. Tertiary phosphines in reactions with substituted cinnamic acids. *J. Organomet. Chem.* **2020**, *910*, 121130. [[CrossRef](#)]
24. Silva, A.T.; Bento, C.M.; Pena, A.C.; Figueiredo, L.M.; Prudêncio, C.; Aguiar, L.; Silva, T.; Ferraz, R.; Gomes, M.S.; Teixeira, C.; et al. Cinnamic Acid Conjugates in the Rescuing and Repurposing of Classical Antimalarial Drugs. *Molecules* **2020**, *25*, 66. [[CrossRef](#)]
25. Shang, H.; Li, L.; Ma, L.; Tian, Y.; Jia, H.; Zhang, T.; Yu, M.; Zou, Z. Design and Synthesis of Molecular Hybrids of Sophora Alkaloids and Cinnamic Acids as Potential Antitumor Agents. *Molecules* **2020**, *25*, 1168. [[CrossRef](#)] [[PubMed](#)]
26. Zhang, J.; Li, N.; Zhang, D.; Dong, M.; Wang, C.; Chen, Y. Construction of cinnamic acids derived β -cyclodextrins and their emodin-based inclusions with enhanced water solubility, excellent antioxidant and antibacterial activities. *Colloids Surf. A* **2020**, *606*, 125382. [[CrossRef](#)]
27. Chen, L.; Zhang, L.; Yan, G.; Huang, D. Recent Advances of Cinnamic Acids in Organic Synthesis. *Asian J. Org. Chem.* **2020**, *9*, 842–862. [[CrossRef](#)]
28. Kumar, A.; Singh, B.K.; Tyagi, R.; Jain, S.K.; Sharma, S.K.; Prasad, A.K.; Raj, H.G.; Rastogi, R.C.; Watterson, A.C.; Parmar, V.S. Mechanism of biochemical action of substituted 4-methylcoumarins. Part 11: Comparison of the specificities of acetoxy derivatives of 4-methylcoumarin and 4-phenylcoumarin to acetoxy coumarins: Protein transacetylase. *Bioorg. Med. Chem.* **2005**, *13*, 4300–4305. [[CrossRef](#)]
29. Zaki, I.; Ramadan, H.M.M.; El-Sayed, E.-S.H.; El-Moneim, M.A. Design, synthesis, and cytotoxicity screening of new synthesized imidazolidine-2-thiones as VEGFR-2 enzyme inhibitors. *Arch. Pharm.* **2020**, *353*, 2000121. [[CrossRef](#)]
30. Kattan, S.W.; Nafie, M.S.; Elmgeed, G.A.; Alelwani, W.; Badar, M.; Tantawy, M.A. Molecular docking, anti-proliferative activity and induction of apoptosis in human liver cancer cells treated with androstane derivatives: Implication of PI3K/AKT/mTOR pathway. *J. Steroid Biochem. Mol. Biol.* **2020**, *198*, 1–9. [[CrossRef](#)]
31. Shukla, S.; Srivastava, R.S.; Shrivastava, S.K.; Sodhi, A.; Kumar, P. Synthesis, cytotoxic evaluation, docking and in silico pharmacokinetic prediction of 4-arylideneamino/cycloalkylideneamino 1, 2-naphthoquinone thiosemicarbazones. *J. Enzyme Inhib. Med. Chem.* **2013**, *28*, 1192–1198. [[CrossRef](#)] [[PubMed](#)]
32. Nafie, M.S.; Tantawy, M.A.; Elmgeed, G.A. Screening of different drug design tools to predict the mode of action of steroidal derivatives as anti-cancer agents. *Steroids* **2019**, *152*, 1–16. [[CrossRef](#)]

33. Tantawy, E.S.; Amer, A.M.; Mohamed, E.K.; Alla, M.M.A.; Nafie, M.S. Synthesis, characterization of some pyrazine derivatives as anti-cancer agents: In vitro and in Silico approaches. *J. Mol. Struct.* **2020**, *1210*, 128013. [[CrossRef](#)]
34. Khodair, A.I.; Alsafi, M.A.; Nafie, M.S. Synthesis, molecular modeling and anti-cancer evaluation of a series of quinazoline derivatives. *Carbohydr. Res.* **2019**, *486*, 07832. [[CrossRef](#)] [[PubMed](#)]
35. Morris, G.M.; Goodsell, D.S.; Halliday, R.S.; Huey, R.; Hart, W.E.; Belew, R.K.; Olson, A.J. Automated docking using a Lamarckian genetic algorithm and an empirical binding free energy function. *J. Comput. Chem.* **1998**, *19*, 1639–1662. [[CrossRef](#)]
36. Solis, F.J.; Wets, R.J.B. Minimization by Random Search Techniques. *Math. Oper. Res.* **1981**, *6*, 19–30. [[CrossRef](#)]
37. Bikadi, Z.; Hazai, E. Application of the PM6 semi-empirical method to modeling proteins enhances docking accuracy of AutoDock. *J. Cheminf.* **2009**, *1*, 15. [[CrossRef](#)] [[PubMed](#)]